

Transport-Equilibrium Schemes for Computing Nonclassical Shocks. Scalar Conservation Laws

Christophe Chalons*

November 20, 2006

Abstract

This paper presents a very efficient numerical strategy for computing the weak solutions of scalar conservation laws which fail to be genuinely nonlinear. We concentrate on the typical situation of either concave-convex or convex-concave flux functions. In such a situation, nonclassical shocks violating the classical Oleinik entropy criterion must be taken into account since they naturally arise as limits of certain diffusive-dispersive regularizations to hyperbolic conservation laws. Such discontinuities play an important part in the resolution of the Riemann problem and their dynamics turns out to be driven by a prescribed *kinetic function* which acts as a selection principle. It aims at imposing the entropy dissipation rate across nonclassical discontinuities, or equivalently their speed of propagation. From a numerical point of view, the serious difficulty consists in enforcing the *kinetic criterion*, that is in controlling the numerical entropy dissipation of the nonclassical shocks for any given discretization. This is known to be a very challenging issue. By means of an algorithm made of two steps, namely an *Equilibrium step* and a *Transport step*, we show how to force the validity of the *kinetic criterion* at the discrete level. The resulting scheme provides in addition sharp profiles. Numerical evidences illustrate the validity of our approach.

1 Introduction

We are interested in computing nonclassical weak solutions of an initial-value problem for a scalar conservation law of the form

$$\begin{cases} \partial_t u + \partial_x f(u) = 0, & u(x, t) \in \mathbb{R}, \quad x \in \mathbb{R}, \quad t > 0, \\ u(x, 0) = u_0(x), \end{cases} \quad (1)$$

where t is the time, x is the one dimensional space variable and $f : \mathbb{R} \rightarrow \mathbb{R}$ is a smooth flux-function neither convex nor concave. Generally speaking, it is well-known that due to the non-linearity of f , solutions of problem (1) may develop discontinuities in finite time and so, are not uniquely determined by initial data u_0 . To overcome this difficulty, solutions of (1) may be asked to satisfy, according to a diffusive regularization principle, a full set of entropy inequalities of the form

$$\partial_t U(u) + \partial_x F(u) \leq 0, \quad \forall (U, F), \quad (2)$$

where $U : \mathbb{R} \rightarrow \mathbb{R}$ and $F : \mathbb{R} \rightarrow \mathbb{R}$ are *unspecified* (smooth) functions such that U is convex and $F' = U' f'$. We recall that an equivalent formulation of this selection principle stipulates that

*Université Paris 7 & Laboratoire JLL, U.M.R. 7598, Boîte courrier 187, 75252 Paris Cedex 05, France. E-mail: chalons@math.jussieu.fr

any shock wave solution of (1), separating two constant states u_- and u_+ and propagating with speed σ given by Rankine-Hugoniot conditions, that is

$$u(x, t) = \begin{cases} u_- & \text{if } x < \sigma t, \\ u_+ & \text{if } x > \sigma t, \end{cases} \quad \text{with } \sigma = \sigma(u_-, u_+) = \frac{f(u_+) - f(u_-)}{u_+ - u_-}, \quad (3)$$

must satisfy Oleinik's entropy inequalities

$$\frac{f(v) - f(u_-)}{v - u_-} \geq \frac{f(u_+) - f(u_-)}{u_+ - u_-}, \quad \text{for all } v \text{ between } u_- \text{ et } u_+. \quad (4)$$

In addition, note that selection principles (2) and (4) imply the Lax shock inequalities

$$f'(u_-) \geq \sigma \geq f'(u_+). \quad (5)$$

We refer the reader to [16] for additional details. When more general regularizations including diffusive *and* dispersive terms are considered, solutions of (1) are asked to obey only a single entropy inequality of the form

$$\partial_t U(u) + \partial_x F(u) \leq 0, \quad (6)$$

where $U : \mathbb{R} \rightarrow \mathbb{R}$ and $F : \mathbb{R} \rightarrow \mathbb{R}$ are now *specified* (smooth) functions, such that U is strictly convex and $F' = U' f'$.

When f is convex or concave, it turns out that all of the entropy conditions (2)-(4)-(5)-(6) are equivalent and actually select a unique *classical* solution of the Riemann problem associated with (1), that is when considering a particular initial data of the form

$$u_0(x) = \begin{cases} u_l & \text{if } x < 0, \\ u_r & \text{if } x > 0, \end{cases} \quad (7)$$

with u_l and u_r two constant states in \mathbb{R} . However, the situation becomes more complicated when f fails to be either convex or concave. In such a situation, while conditions (2) and (4) still select equivalently a unique *classical* solution of (1)-(7), it is necessary to supplement the Riemann problem (1)-(7) with an additional selection criterion when the single entropy inequality (6) only is imposed on the solutions. This criterion is called *kinetic relation* from [16]. Basically, there exists many discontinuous solutions (more precisely a one-parameter family of solutions) to the Riemann problem (1)-(6)-(7), all of them except the *classical* one containing a shock wave violating the Lax shock inequalities (5). Such discontinuities are often referred as to *undercompressive shocks* or *nonclassical shocks*, and sometimes as to *phase transitions* depending on the context.

In order for the uniqueness of the entropy solution of the Riemann problem (1)-(6)-(7) to be ensured, a *kinetic relation* needs to be added along each nonclassical discontinuity connecting a left hand state u_- to a right hand state u_+ . It aims at imposing the rate of entropy dissipation (6) across the admissible nonclassical discontinuities, or equivalently their speed of propagation. Usually, the *kinetic criterion* takes the form

$$u_+ = \varphi^b(u_-) \quad \text{or} \quad u_- = \varphi^{-b}(u_+) \quad \text{for all nonclassical shocks,} \quad (8)$$

where φ^b is the so-called *kinetic function* and φ^{-b} its inverse. Again, we refer the reader to [16] for a general theory of nonclassical entropy solutions supplemented with a kinetic relation.

The numerical approximation of nonclassical solutions is known to be very challenging and still constitutes an open problem. The main difficulty is related to the respect of the kinetic

relation at the discrete level. Basically, two strategies exist to approach this problem. The first one tries to impose the kinetic relation by taking into account the associated small scales, that is the diffusive and dispersive terms that actually generate nonclassical solutions. It amounts to propose a scheme whose equivalent equation best looks like the regularized model with diffusive and dispersive terms. This is usually achieved by means of entropy stable and high-order accurate techniques. In practice, this method provides satisfactory results for shocks with *small strength*, but shocks with *large strength* are not properly captured due to the great sensitivity of the nonclassical shocks with respect to the numerical diffusion and small scales in general. For more details, we refer for instance to [10], [11], [17], [6], [7] or [3] and the references therein. The second strategy, known under the name of "sharp interface approach", deals directly with the kinetic function φ^b to tackle the dynamics of the nonclassical solutions. In this context, the front tracking scheme and Glimm's random choice scheme are free of artificial numerical diffusion and then give *sharp* nonclassical shocks satisfying the prescribed kinetic relation. But these methods actually rely on the knowledge of the underlying nonclassical Riemann solution, which prevents any complex application. See for instance [15], [8], [1], [12], [13].

In this paper, we present a new scheme based on a "sharp interface approach" for capturing discontinuities whose dynamics is driven by a prescribed kinetic function. By construction, our scheme gives sharp isolated nonclassical shocks, but contrarily to Glimm's random choice scheme for instance it does not explicitly use the solution of the corresponding nonclassical Riemann solver. The resulting algorithm is essentially conservative and provides numerical results in full agreement with exact ones, whatever the strength of the shocks are. In some sense, our algorithm keeps the advantages of Glimm's random choice scheme (sharp interfaces propagating at the right speed) and leaves its main drawbacks (the need of the nonclassical Riemann solutions).

2 Nonclassical Riemann solvers for concave-convex and convex-concave flux functions

In this section, we follow [16] and review the theory of nonclassical Riemann solutions to (1)-(6)-(7)-(8) in the non restrictive situation when the flux function f is either concave-convex, in the sense that

$$\begin{aligned} u f''(u) > 0 \quad \text{when } u \neq 0, \quad f'''(0) \neq 0, \\ \text{and } \lim_{|u| \rightarrow +\infty} f'(u) = +\infty, \end{aligned} \tag{9}$$

or convex-concave in the sense that

$$\begin{aligned} u f''(u) < 0 \quad \text{when } u \neq 0, \quad f'''(0) \neq 0, \\ \text{and } \lim_{|u| \rightarrow +\infty} f'(u) = -\infty. \end{aligned} \tag{10}$$

Such flux functions have an unique inflection point at $u = 0$. Typically, we will consider the two cases $f(u) = u^3$ and $f(u) = -u^3$ in Section 4 devoted to the numerical experiments.

Following [16], we first define the function $\varphi^{\natural} : \mathbb{R} \rightarrow \mathbb{R}$ related to the graph of f in the (u, f) -plane as follows : for any $u \neq 0$, $\varphi^{\natural}(u) \neq u$ is the unique value such that the line passing through the points $(u, f(u))$ and $(\varphi^{\natural}(u), f(\varphi^{\natural}(u)))$ is tangent to the graph of f at point $(\varphi^{\natural}(u), f(\varphi^{\natural}(u)))$:

$$f'(\varphi^{\natural}(u)) = \frac{f(u) - f(\varphi^{\natural}(u))}{u - \varphi^{\natural}(u)}.$$

Setting $\varphi^{\natural}(0) = 0$, the function $\varphi^{\natural} : \mathbb{R} \rightarrow \mathbb{R}$ is seen to be smooth, monotone decreasing and onto thanks to (9) or (10). We denote $\varphi^{-\natural} : \mathbb{R} \rightarrow \mathbb{R}$ its inverse function. It turns out that φ^{\natural} and

$\varphi^{-\sharp}$ play an important role when addressing the single entropy inequality (6) for discontinuous solutions. More precisely, considering a shock wave solution of (1) of the form (3), the entropy inequality (6) holds in the integral sense if and only if the entropy dissipation

$$E(u_-, u_+) = -\sigma(u_-, u_+)(U(u_+) - U(u_-)) + (F(u_+) - F(u_-))$$

is such that $E(u_-, u_+) \leq 0$. It is proved in [16] that the function $u_+ \rightarrow E(u_-, u_+)$ achieves a maximum negative (respectively positive) value at $u_+ = \varphi^\sharp(u_-)$ when f is concave-convex (respectively convex-concave), while vanishing exactly twice at u_- and let us say $\varphi_0^\flat(u_-) \in [\varphi^{-\sharp}(u_-), \varphi^\sharp(u_-)]$. Moreover, assuming that $u_- > 0$ we have $E(u_-, u_+) < 0$ if $u_+ \in (\varphi_0^\flat(u_-), \varphi^\sharp(u_-))$ (respectively $u_+ \in (\varphi^{-\sharp}(u_-), \varphi_0^\flat(u_-))$) when f is concave-convex (respectively convex-concave). This will motivate assumptions (11) and (12) made on the kinetic function φ^b applied to select the nonclassical shock waves. Let us now give the nonclassical Riemann solver associated with (1)-(6)-(7)-(8), see [16].

The case of a concave-convex flux function :

Let us assume that f obeys (9) and let $\varphi^b : \mathbb{R} \rightarrow \mathbb{R}$ be a kinetic function, that is (by definition) a monotone decreasing and Lipschitz continuous mapping such that

$$\begin{cases} \varphi_0^\flat(u) < \varphi^b(u) \leq \varphi^\sharp(u) & \text{if } u > 0, \\ \varphi^\sharp(u) \leq \varphi^b(u) < \varphi_0^\flat(u) & \text{if } u < 0. \end{cases} \quad (11)$$

From φ^b , we define the function $\varphi^\sharp : \mathbb{R} \rightarrow \mathbb{R}$ such that the line passing through the points $(u, f(u))$ and $(\varphi^b(u), f(\varphi^b(u)))$ with $u \neq 0$ also cuts the graph of the flux function f at point $(\varphi^\sharp(u), f(\varphi^\sharp(u)))$ with $\varphi^\sharp(u) \neq u$ and $\varphi^\sharp(u) \neq \varphi^b(u)$:

$$\frac{f(u) - f(\varphi^b(u))}{u - \varphi^b(u)} = \frac{f(u) - f(\varphi^\sharp(u))}{u - \varphi^\sharp(u)}.$$

Then, the nonclassical Riemann solver associated with (1)-(6)-(7)-(8) is given as follows.

When $u_l > 0$:

- (1) If $u_r \geq u_l$, the solution is a rarefaction wave connecting u_l to u_r .
- (2) If $u_r \in [\varphi^\sharp(u_l), u_l)$, the solution is a classical shock wave connecting u_l to u_r .
- (3) If $u_r \in (\varphi^b(u_l), \varphi^\sharp(u_l))$, the solution contains a nonclassical shock connecting u_l to $\varphi^b(u_l)$, followed by a classical shock connecting $\varphi^b(u_l)$ to u_r .
- (4) If $u_r \leq \varphi^b(u_l)$, the solution contains a nonclassical shock connecting u_l to $\varphi^b(u_l)$, followed by a rarefaction connecting $\varphi^b(u_l)$ to u_r .

When $u_l \leq 0$:

- (1) If $u_r \leq u_l$, the solution is a rarefaction wave connecting u_l to u_r .
- (2) If $u_r \in [u_l, \varphi^\sharp(u_l))$, the solution is a classical shock wave connecting u_l to u_r .
- (3) If $u_r \in (\varphi^\sharp(u_l), \varphi^b(u_l))$, the solution contains a nonclassical shock connecting u_l to $\varphi^b(u_l)$, followed by a classical shock connecting $\varphi^b(u_l)$ to u_r .
- (4) If $u_r \geq \varphi^b(u_l)$, the solution contains a nonclassical shock connecting u_l to $\varphi^b(u_l)$, followed by a rarefaction connecting $\varphi^b(u_l)$ to u_r .

The case of a convex-concave flux function :

Let us assume that f obeys (10) and let $\varphi^b : \mathbb{R} \rightarrow \mathbb{R}$ be a kinetic function, that is (again by definition) a monotone decreasing and Lipschitz continuous mapping such that

$$\begin{cases} \varphi_0^\flat(u) < \varphi^b(u) \leq \varphi^{-\sharp}(u) & \text{if } u < 0, \\ \varphi^{-\sharp}(u) \leq \varphi^b(u) < \varphi_0^\flat(u) & \text{if } u > 0. \end{cases} \quad (12)$$

We then define $\rho(u, v) \in \mathbb{R}$ if $v \neq u$ and $v \neq \varphi^b(u)$ by

$$\frac{f(\rho(u, v)) - f(u)}{\rho(u, v) - u} = \frac{f(v) - f(u)}{v - u}$$

with $\rho(u, v) \neq u$ and $\rho(u, v) \neq v$, and extend the function ρ by continuity otherwise. Of course, we note that $\varphi^\sharp(u) = \rho(u, \varphi^b(u))$ where φ^\sharp is defined as in the case of a concave-convex flux function.

Then, the nonclassical Riemann solver associated with (1)-(6)-(7)-(8) is given as follows.

When $u_l > 0$:

- (1) If $u_r \geq u_l$, the solution is a classical shock connecting u_l to u_r .
- (2) If $u_r \in [0, u_l)$, the solution is a rarefaction wave connecting u_l to u_r .
- (3) If $u_r \in (\varphi^b(u_l), 0)$, the solution contains a rarefaction wave connecting u_l to $\varphi^{-b}(u_r)$, followed by a nonclassical shock connecting $\varphi^{-b}(u_r)$ to u_r .
- (4) If $u_r \leq \varphi^b(u_l)$, the solution contains :
 - (i) a classical shock connecting u_l to $\varphi^{-b}(u_r)$, followed by a nonclassical shock connecting $\varphi^{-b}(u_r)$ to u_r , if $u_l > \rho(\varphi^{-b}(u_r), u_r)$.
 - (ii) a classical shock connecting u_l to u_r , if $u_l \leq \rho(\varphi^{-b}(u_r), u_r)$.

When $u_l \leq 0$:

- (1) If $u_r \leq u_l$, the solution is a classical shock connecting u_l to u_r .
- (2) If $u_r \in (u_l, 0]$, the solution is a rarefaction wave connecting u_l to u_r .
- (3) If $u_r \in (0, \varphi^b(u_l))$, the solution contains a rarefaction wave connecting u_l to $\varphi^{-b}(u_r)$, followed by a non classical shock connecting $\varphi^{-b}(u_r)$ to u_r .
- (4) If $u_r \geq \varphi^b(u_l)$, the solution contains :
 - (i) a classical shock connecting u_l to $\varphi^{-b}(u_r)$, followed by a nonclassical shock connecting $\varphi^{-b}(u_r)$ to u_r , if $u_l < \rho(\varphi^{-b}(u_r), u_r)$.
 - (ii) a classical shock connecting u_l to u_r , if $u_l \geq \rho(\varphi^{-b}(u_r), u_r)$.

3 Numerical approximation

In this section, we present a suitable algorithm for approximating the nonclassical Riemann solutions of (1)-(6)-(7)-(8). Let us first introduce some notations. We assume as given a constant time step Δt and a constant space step Δx , and we denote $x_{j+1/2} = j\Delta x$ for $j \in \mathbb{Z}$ the interfaces and $t^n = n\Delta t$ for $n \in \mathbb{N}$ the intermediate times. Then, we seek at each time t^n a constant approximation u_j^n of the solution $x \rightarrow u(x, t^n)$ on each interval $C_j = [x_{j-1/2}; x_{j+1/2}[$ and for all $j \in \mathbb{Z}$.

From the previous sections, it is clear that most of the theoretical as well as numerical difficulties are a direct consequence of the existence of two areas having different convexity properties on the graph of the flux function f . That is the reason why we will only focus ourselves, in a first approach at least (see indeed Section 5 for the general case), on the most difficult solutions to capture numerically, that is those joining areas having a different convexity. When f obeys either (9) or (10), it is a matter of solutions separating two states u_- and u_+ such that $u_- u_+ < 0$. Concerning the solutions remaining always either in \mathbb{R}^- or \mathbb{R}^+ , we choose from now on a numerical flux function g consistent with the flux function f and we will consider in this case the following 3-point explicit conservative scheme to numerically solve (1):

$$u_j^{n+1} = u_j^n - \lambda(g_{j+1/2} - g_{j-1/2}), \quad g_{j+1/2} = g(u_j^n, u_{j+1}^n), \quad j \in \mathbb{Z}, \quad (13)$$

with $\lambda = \frac{\Delta t}{\Delta x}$ defined under the usual CFL restriction

$$\lambda \max_u |f'(u)| \leq \frac{1}{2} \quad (14)$$

for all the u under consideration. We have $g(u, u) = f(u) \forall u$ by consistency of g . The question is now to understand how to modify such a conservative scheme in order to properly capture all the solutions of the Riemann problem (1)-(6)-(7)-(8), that is including those associated with the case $u_l u_r < 0$ in (7). Note from now on that the proposed modification is still going to use the function g but *not* in the same way as in (13).

With this in mind, let us introduce two subsets \mathcal{C} and \mathcal{N} made of all the pairs $(u_l, u_r) \in \mathbb{R}^2$ with $u_l u_r < 0$ (the most interesting situation) and such that the Riemann solution of (1)-(6)-(7)-(8) is respectively classical and nonclassical. In view of the previous section, we thus have

$$\mathcal{C} = \quad (15)$$

$$\left| \begin{array}{l} \{(u_l, u_r), u_l u_r < 0 / u_l u_r \geq u_l \varphi^\sharp(u_l)\} \text{ if } f \text{ obeys (9),} \\ \{(u_l, u_r), u_l u_r < 0 / u_l u_r \leq u_l \varphi^b(u_l) \text{ and } u_l^2 \leq u_l \rho(\varphi^{-b}(u_r), u_r)\} \text{ if } f \text{ obeys (10),} \end{array} \right.$$

and

$$\mathcal{N} = \quad (16)$$

$$\left| \begin{array}{l} \{(u_l, u_r), u_l u_r < 0 / u_l u_r < u_l \varphi^\sharp(u_l)\} \text{ if } f \text{ obeys (9),} \\ \{(u_l, u_r), u_l u_r < 0 / \{u_l u_r > u_l \varphi^b(u_l)\} \text{ or } \{u_l u_r \leq u_l \varphi^b(u_l) \text{ and } u_l^2 > u_l \rho(\varphi^{-b}(u_r), u_r)\} \} \text{ if } f \text{ obeys (10).} \end{array} \right.$$

We now assume that $u \varphi^\sharp(u) < 0$ for all u so that \mathcal{C} is not an empty set. This assumption is classical (and turns out to be fulfilled in most situations of interest) and the consequence is that the Riemann solution is always *classical* when the initial data belongs to the same region of convexity or concavity of f . Moreover, the Riemann solution associated with a pair (u_l, u_r) in \mathcal{C} is always a classical shock connecting u_l to u_r while if (u_l, u_r) belongs to \mathcal{N} , the Riemann solution is nonclassical and composite (made of two waves) except if $u_r = \varphi^b(u_l)$. In the latter case, the solution simply consists of a nonclassical shock from u_l to u_r since the kinetic criterion is respected.

3.1 Motivations

We begin by explaining the two basic motivations that will eventually lead to the definition of our algorithm. Namely : to eliminate the spurious intermediate points in numerical shock waves (classical or nonclassical) joining two regions of different convexity of f , and to properly capture the nonclassical shock waves.

First of all, let us consider a Riemann initial data (7) such that $u_l u_r < 0$ and the corresponding Riemann solution of (1)-(6)-(7)-(8) is a non trivial shock wave (either classical if $(u_l, u_r) \in \mathcal{C}$ or nonclassical if $(u_l, u_r) \in \mathcal{N}$) from u_l to u_r and propagating at speed $\sigma(u_l, u_r)$ given by the Rankine-Hugoniot relation :

$$\sigma(u, v) = \frac{f(u) - f(v)}{u - v}, \quad \forall u \neq v. \quad (17)$$

Let us assume moreover that $\sigma(u_l, u_r) \neq 0$. We observe in this situation that any given conservative scheme (13) generally creates spurious values distinct from u_l and u_r from the first time iteration - and we will see in Section 4 devoted to the numerical experiments that when the

shock is nonclassical $((u_l, u_r) \in \mathcal{N})$, these spurious values "propagate" from a time iteration to another, leading eventually to a numerical solution in full disagreement with the exact one -. Indeed, considering the following natural discretization of (7)

$$u_j^0 = \begin{cases} u_l & \text{if } j \leq 0, \\ u_r & \text{if } j \geq 1, \end{cases} \quad (18)$$

we get

$$u_j^1 = \begin{cases} u_l - \lambda(g(u_l, u_l) - g(u_l, u_l)) = u_l & \text{if } j \leq -1, \\ u_l - \lambda(g(u_l, u_r) - g(u_l, u_l)) & \text{if } j = 0, \\ u_r - \lambda(g(u_r, u_r) - g(u_l, u_r)) & \text{if } j = 1, \\ u_r - \lambda(g(u_r, u_r) - g(u_r, u_r)) = u_r & \text{if } j \geq 2. \end{cases}$$

Then, we have $u_0^1 \notin \{u_l, u_r\}$ or $u_1^1 \notin \{u_l, u_r\}$ as soon as λ is different from $|1/\sigma(u_l, u_r)| = |u_r - u_l|/|f(u_r) - f(u_l)|$. Indeed, if we assume for instance that $u_0^1 = u_l$ (the other cases are similar) then it means that $g(u_l, u_r) = g(u_l, u_l) = f(u_l)$ so that $u_1^1 = u_r - \lambda(f(u_r) - f(u_l))$. This quantity is actually distinct from u_l and u_r if λ is not equal to $|1/\sigma(u_l, u_r)|$.

Instead, we would prefer to keep a sharp interface between u_l and u_r , propagating at speed $\sigma(u_l, u_r)$. In order to achieve this goal, we propose to replace (13) with an update formula defined in two steps.

One of these steps (the Equilibrium step) proposes to keep the "equilibrium relation" existing at the interface between u_l and u_r . By "equilibrium relation" we mean that u_l and u_r (the left and the right states of the interface $x_{1/2}$) are not in the same region of convexity of the flux function *but* can be joined by an admissible discontinuity. Recall that this discontinuity is classical if $(u_l, u_r) \in \mathcal{C}$ and nonclassical if $(u_l, u_r) \in \mathcal{N}$. For that, we propose to replace the numerical flux $g_{1/2}$ with a left (respectively right) numerical flux $g_{1/2}^L$ (respectively $g_{1/2}^R$) in the calculation of u_0^1 (respectively u_1^1) when setting now

$$\begin{cases} u_0^1 = u_l - \lambda(g_{1/2}^L - g(u_l, u_l)), \\ u_1^1 = u_r - \lambda(g(u_r, u_r) - g_{1/2}^R). \end{cases} \quad (19)$$

These two numerical fluxes are defined so as to maintain the equilibrium relation as follows

$$g_{1/2}^L = g(u_l, u_r^-), \quad g_{1/2}^R = g(u_l^+, u_r),$$

where the so-called equilibrium states u_r^- and u_l^+ are defined according to the relations

$$u_r^- = u_r^-(u_l, u_r) = u_l \quad \text{and} \quad u_l^+ = u_l^+(u_l, u_r) = u_r \quad \text{if } (u_l, u_r) \in \mathcal{C},$$

and

$$u_r^- = \varphi^{-1}(u_r)(= u_l) \quad \text{and} \quad u_l^+ = \varphi(u_l)(= u_r) \quad \text{if } (u_l, u_r) \in \mathcal{N}.$$

This strategy is similar to the one used in the definition of well-balanced schemes for conservation laws with source terms (balance laws). See for instance [2] and the now large literature on this subject. Then, we get by (19)

$$\begin{cases} u_0^1 = u_l - \lambda(g(u_l, u_l) - g(u_l, u_l)) = u_l, \\ u_1^1 = u_r - \lambda(g(u_r, u_r) - g(u_r, u_r)) = u_r. \end{cases}$$

Thanks to the new update formula (19), we are thus able to remove the undesired values. Nevertheless, it is clear at this stage that the initial discretization (18) is made stationary by

this new update formula, when it should be moving at speed $\sigma(u_l, u_r)$. A transport step must thus be included in our algorithm. This step (the Transport step) proposes to take into account the dynamics of the discontinuity left stationary in the Equilibrium step. In order to avoid the emergence of new spurious values, we will make use of a random sampling strategy. The full description is proposed in the next subsection.

The second motivation in the installation of our algorithm concerns the situation where a nonclassical shock (which is not present in the initial data) is generated by the nonclassical Riemann solver. That corresponds to the situation $(u_l, u_r) \in \mathcal{N}$ and $u_r \neq \varphi(u_l)$. We would like to force the numerical scheme to create this nonclassical discontinuity. Well, the same two-step strategy will be used, namely a step where the numerical flux $g(u_l, u_r)$ is splitted into two fluxes $g^L(u_l, u_r^-)$ and $g^R(u_l^+, u_r)$ (with $u_r^- = \varphi^{-1}(u_r)$ and $u_l^+ = \varphi(u_l)$) in order to enforce an equilibrium relation at the corresponding interface, and an other step to make moving the corresponding nonclassical discontinuity.

3.2 Numerical algorithm

We describe in this section our algorithm in details. As motivated above, the method is made of two steps : an *Equilibrium step* and a *Transport step*. In the equilibrium step, we propose to modify any conservative scheme of the form (13) in order to create an equilibrium relation at each interface $x_{j+1/2}$ such that $u_j u_{j+1} < 0$. The Transport step aims at propagating the corresponding discontinuities. We propose to define our algorithm when starting with the Transport step and to follow with the Equilibrium step. It is worth noticing from now on that the resulting scheme really uses few things coming from the nonclassical Riemann solver, namely only informations concerning the appearance of nonclassical shocks via the sets \mathcal{C} and \mathcal{N} . But in no way the Riemann solution itself. That represents a considerable profit compared to Glimm's random choice scheme for instance.

Assuming as given u_{j-1}^n , u_j^n and u_{j+1}^n , we show now how to define u_j^{n+1} . Note that, under the CFL condition (14), it is sufficient to focus our reasoning on the interval $[x_{j-1}, x_{j+1}]$, since the Riemann problems set at other interfaces are not expected to influence the definition of u_j^{n+1} .

First step ($t^n \rightarrow t^{n+1/2}$)

This step is concerned with the dynamics of the admissible discontinuities (classical or nonclassical) joining the two regions of different convexity of f . In the next Equilibrium step, these discontinuities will then be left stationary. We first recall that the speed of propagation $\sigma(u_-, u_+)$ of an admissible discontinuity between u_- and u_+ is given by the Rankine-Hugoniot relation (17). Our aim is to get for all j a new approximation $u_j^{n+1/2}$ at time $t^{n+1/2} = t^n + \Delta t$. For that we introduce the following function (see also figure 1) defined on the interval $[x_{j-1}, x_{j+1}]$:

$$v(x, t) = \begin{cases} u_{j-1}^n & \text{if } x \in [x_{j-1}, x_{j-1/2}[, \\ u_j^{n,-} & \text{if } x \in [x_{j-1/2}, x_{j-1/2} + \sigma_{j-1/2}^+ \Delta t[, \\ u_j^n & \text{if } x \in [x_{j-1/2} + \sigma_{j-1/2}^+ \Delta t, x_{j+1/2} + \sigma_{j+1/2}^- \Delta t[, \\ u_j^{n,+} & \text{if } x \in [x_{j+1/2} + \sigma_{j+1/2}^- \Delta t, x_{j+1/2}[, \\ u_{j+1}^n & \text{if } x \in [x_{j+1/2}, x_{j+1}] , \end{cases} \quad (20)$$

with $\sigma_{j+1/2}^- = \min(\sigma_{j+1/2}, 0)$ and $\sigma_{j-1/2}^+ = \max(\sigma_{j-1/2}, 0)$. This function proposes to make enter the cell \mathcal{C}_j a discontinuity from the interface $x_{j-1/2}$ (respectively $x_{j+1/2}$) between u_j^n and its equilibrium state $u_j^{n,-}$ (respectively $u_j^{n,+}$) if the corresponding speed of propagation $\sigma_{j-1/2}$ (respectively $\sigma_{j+1/2}$) given by the Rankine-Hugoniot condition is positive (respectively negative).

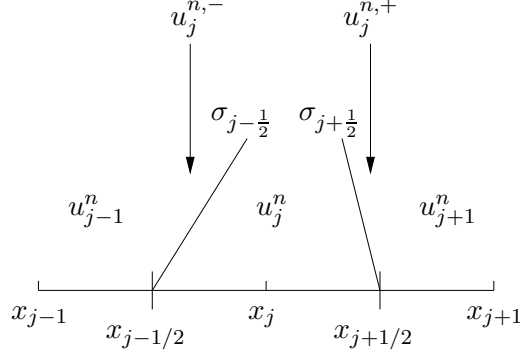


Figure 1: Definition of $v(x, t)$.

The definition of the equilibrium states $u_j^{n,-}$ and $u_j^{n,+}$ depends on u_{j-1}^n , u_j^n and u_{j+1}^n :

- if $(u_{j-1}^n, u_j^n) \in \mathcal{C}$ (respectively $(u_j^n, u_{j+1}^n) \in \mathcal{C}$), u_{j-1}^n and u_j^n (respectively u_j^n and u_{j+1}^n) do not belong to the same region of convexity of f and are joined by a classical shock. Then, the equilibrium state $u_j^{n,-}$ (respectively $u_j^{n,+}$) of u_j^n is simply u_{j-1}^n (respectively u_{j+1}^n), and we set $\sigma_{j\pm 1/2} = \sigma(u_j^n, u_j^{n,\pm})$.
- if $(u_{j-1}^n, u_j^n) \in \mathcal{N}$ (respectively $(u_j^n, u_{j+1}^n) \in \mathcal{N}$), u_{j-1}^n and u_j^n (respectively u_j^n and u_{j+1}^n) do not belong to the same region of convexity of f and the corresponding Riemann solution contains a nonclassical shock satisfying the kinetic relation $u_+ = \varphi(u_-) \iff u_- = \varphi^{-1}(u_+)$ (if u_- and u_+ denote the left and right states of the nonclassical discontinuity). For the equilibrium states, we propose to set (in agreement with the above motivations)

$$u_j^{n,-} = \varphi^{-1}(u_j^n), \quad u_j^{n,+} = \varphi(u_j^n),$$

and again $\sigma_{j\pm 1/2} = \sigma(u_j^n, u_j^{n,\pm})$. Note that these equilibrium states are the expected ones if we have $u_j^n = \varphi(u_{j-1}^n)$ (respectively $u_{j+1}^n = \varphi(u_j^n)$).

- otherwise, u_{j-1}^n and u_j^n (respectively u_j^n and u_{j+1}^n) belong to the same region of convexity of f . Since our objective is to keep on using the usual conservative scheme (13) without modification in such a situation, we simply set $\sigma_{j\pm 1/2} = 0$ so that it is not necessary to define the equilibrium states $u_j^{n,\pm}$ (see again figure 1).

In order to get a new approximation $u_j^{n+1/2}$ at time $t^{n+1/2}$, we propose to define $x \rightarrow v(x, t^{n+1/2})$ by picking randomly in the interval $[x_{j-1/2}, x_{j+1/2}[$ a value from the ones taken by the function (20) at time Δt . More precisely, given a well distributed random sequence (a_n) within interval $(0, 1)$, it amounts to set :

$$v(x, t^{n+1/2}) = \begin{cases} u_{j-1}^n & \text{if } x \in [x_{j-1}, x_{j-1/2}[, \\ u_j^{n+1/2} & \text{if } x \in [x_{j-1/2}, x_{j+1/2}[, \\ u_{j+1}^n & \text{if } x \in [x_{j+1/2}, x_{j+1}], \end{cases} \quad (21)$$

with

$$u_j^{n+1/2} = \begin{cases} u_j^{n,-} & \text{if } a_{n+1} \in (0, \lambda\sigma_{j-1/2}^+), \\ u_j^n & \text{if } a_{n+1} \in [\lambda\sigma_{j-1/2}^+, 1 + \lambda\sigma_{j+1/2}^-), \\ u_j^{n,+} & \text{if } a_{n+1} \in [1 + \lambda\sigma_{j+1/2}^-, 1). \end{cases} \quad (22)$$

See figure 2.

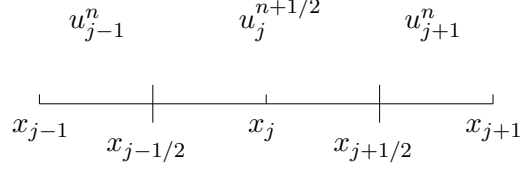


Figure 2: Definition of $v(x, t^{n+1/2})$.

Second step ($t^{n+1/2} \rightarrow t^{n+1}$)

In this step, we consider the following nonconservative formula :

$$u_j^{n+1} = u_j^{n+1/2} - \lambda(g_{j+1/2}^L - g_{j-1/2}^R), \quad j \in \mathbb{Z}, \quad (23)$$

where the numerical fluxes $g_{j+1/2}^L$ and $g_{j-1/2}^R$ are defined as follows

$$g_{j+1/2}^L = g(u_j^{n+1/2}, u_{j+1}^{n+1/2,-}), \quad g_{j-1/2}^R = g(u_{j-1}^{n+1/2,+}, u_j^{n+1/2}). \quad (24)$$

The definition of the equilibrium states $u_{j-1}^{n+1/2,+}$ and $u_{j+1}^{n+1/2,-}$ now depends on u_{j-1}^n , $u_j^{n+1/2}$ and u_{j+1}^n and is proposed in agreement with the first step, namely :

- if $(u_j^{n+1/2}, u_{j+1}^n) \in \mathcal{C}$ (respectively $(u_{j-1}^n, u_j^{n+1/2}) \in \mathcal{C}$), $u_j^{n+1/2}$ and u_{j+1}^n (respectively u_{j-1}^n and $u_j^{n+1/2}$) do not belong to the same region of convexity of f and are joined by a classical shock. Then, the equilibrium state $u_{j+1}^{n+1/2,-}$ (respectively $u_{j-1}^{n+1/2,+}$) of u_{j+1}^n (respectively u_{j-1}^n) is simply $u_j^{n+1/2}$.
- if $(u_j^{n+1/2}, u_{j+1}^n) \in \mathcal{N}$ (respectively $(u_{j-1}^n, u_j^{n+1/2}) \in \mathcal{N}$), $u_j^{n+1/2}$ and u_{j+1}^n (respectively u_{j-1}^n and $u_j^{n+1/2}$) do not belong to the same region of convexity of f and the corresponding Riemann solution contains a nonclassical shock satisfying the kinetic relation. Then $u_{j-1}^{n+1/2,+} = \varphi(u_{j-1}^n)$, $u_{j+1}^{n+1/2,-} = \varphi^{-1}(u_{j+1}^n)$.
- otherwise, $u_j^{n+1/2}$ and u_{j+1}^n (respectively u_{j-1}^n and $u_j^{n+1/2}$) belong to the same region of convexity of f . In this case, we trust the usual numerical flux function $g_{j+1/2}$ and then we set $u_{j-1}^{n+1/2,+} = u_{j-1}^n$, $u_{j+1}^{n+1/2,-} = u_{j+1}^n$, so that $g_{j+1/2}^L = g(u_j^{n+1/2}, u_{j+1}^n)$ and $g_{j-1/2}^R = g(u_{j-1}^n, u_j^{n+1/2})$.

To summarize, one uses (23) in this second step where the numerical fluxes $g_{j+1/2}^L$ and $g_{j-1/2}^R$ are defined as follows for all $j \in \mathbb{Z}$:

$$\begin{aligned} g_{j+1/2}^L &= g_{j+1/2}^L(u_j^{n+1/2}, u_{j+1}^n) \\ &= \begin{cases} g(u_j^{n+1/2}, u_{j+1}^n) & \text{if } (u_j^{n+1/2}, u_{j+1}^n) \in \mathcal{C}, \\ g(u_j^{n+1/2}, \varphi^{-b}(u_{j+1}^n)) & \text{if } (u_j^{n+1/2}, u_{j+1}^n) \in \mathcal{N}, \\ g(u_j^{n+1/2}, u_{j+1}^n) & \text{otherwise,} \end{cases} \end{aligned} \quad (25)$$

and

$$\begin{aligned}
g_{j-1/2}^R &= g_{j-1/2}^R(u_{j-1}^n, u_j^{n+1/2}) \\
&= \begin{cases} g(u_j^{n+1/2}, u_j^{n+1/2}) & \text{if } (u_{j-1}^n, u_j^{n+1/2}) \in \mathcal{C}, \\ g(\varphi^b(u_{j-1}^n), u_j^{n+1/2}) & \text{if } (u_{j-1}^n, u_j^{n+1/2}) \in \mathcal{N}, \\ g(u_{j-1}^n, u_j^{n+1/2}) & \text{otherwise.} \end{cases} \quad (26)
\end{aligned}$$

This concludes the description of our numerical strategy.

In the next section, we justify the proposed procedure by several numerical experiments. From a theoretical point of view, we are able to prove an important property of "strong" consistency of the method which is the matter of the next statement. By "strong" consistency, we mean that the proposed algorithm preserves the constant states and is convergent in the important case of a solution consisting either in an isolated classical or nonclassical shock or remaining in the same region of convexity or concavity of the flux function. Actually, the convergence of the method in a more general situation remains an open question at the moment.

Theorem 1 (Consistency) *Under the CFL restriction (14), the scheme defined by (23)-(22)-(25)-(26) is consistent with (1)-(6)-(7)-(8) in the following sense :*

(i) Constant state : Assume that $u := u_{j-1}^n = u_j^n = u_{j+1}^n$, then $u_j^{n+1} = u$.

(ii) Isolated classical or nonclassical shock (joining the two regions of different convexity of f) : Let u^l and u^r be two constant states such that $u^l u^r < 0$ and that can be connected by an admissible classical ($(u^l, u^r) \in \mathcal{C}$) or nonclassical ($u^r = \varphi^b(u^l)$) shock. Assume that $u_j^0 = u^l$ if $j \leq 0$ and $u_j^0 = u^r$ if $j \geq 1$. Then the scheme (23)-(22)-(25)-(26) is equivalent to Glimm's random choice scheme and then converges to the solution of (1)-(6)-(7)-(8) given by $u(x, t) = u^l$ if $x < \sigma(u^l, u^r)t$ and $u(x, t) = u^r$ otherwise. In particular, we have $u_j^n \in \{u^l, u^r\} \forall j \in \mathbb{Z}$ and $\forall n \in \mathbb{N}$ so that the discontinuity is sharp.

(iii) Classical solution (remaining in the region of convexity - or concavity - of f) : Let us assume that u_{j-1}^n, u_j^n and u_{j+1}^n are either all non-positive or all non-negative. Then the definition u_j^{n+1} given by (23)-(22)-(25)-(26) coincides with the one given by the usual conservative formula (13). Then it obeys all the stability properties provided by the choice of the flux function g . In particular, the strategy can also be convergent in this situation.

Proof.

(iii) (and (i) as a particular case) If u_{j-1}^n, u_j^n and u_{j+1}^n are either all non-positive or all non-negative, then (u_{j-1}^n, u_j^n) and (u_j^n, u_{j+1}^n) neither belong to \mathcal{C} nor \mathcal{N} . Then, by definition $\sigma_{j-1/2} = \sigma_{j+1/2} = 0$ and (22) implies that $u_j^{n+1/2} = u_j^n$. For the same reason, we get from (25)-(26) that $g_{j+1/2}^L = g_{j+1/2}^L(u_j^{n+1/2}, u_{j+1}^n) = g(u_j^n, u_{j+1}^n)$ and $g_{j-1/2}^R = g_{j-1/2}^R(u_{j-1}^n, u_j^{n+1/2}) = g(u_{j-1}^n, u_j^n)$ and eventually that (23) coincides with (13). The case (i) follows as a particular case of (iii) and from the consistency of g .

(ii) We give the proof in the case of an admissible (classical or nonclassical) shock propagating with a positive speed, *i.e.* $\sigma(u^l, u^r) > 0$ (the case $\sigma(u^l, u^r) \leq 0$ can be treated similarly). Moreover, it is clearly sufficient to prove that our algorithm and Glimm's one coincide for the first time iteration. In the first time iteration, it is clear by (22) and $\sigma(u^l, u^r) > 0$ that $u_j^{1/2} = u_j^0$ for all $j \neq 1$ while for $j = 1$, a value is picked between $u_j^0 = u^r$ and $u^{0,-} = u^l$. This value

is chosen randomly but in agreement with the rate of presence in the cell of u^l and u^r at time Δt , that is in agreement with the speed of propagation $\sigma_{1/2}^+ = \sigma(u^l, u^r)$ of the corresponding discontinuity. See indeed (22) and note that $\sigma_{3/2}^- = 0$ since $u_1^0 = u_2^0 = u^r$. Then it is now clear that the definition of $u_j^{1/2}$ in (22) coincides with the one that would provide the Glimm scheme.

To prove our result, we thus have to show now that $u_j^1 = u_j^{1/2}$ for all j . The non trivial cases are clearly u_0^1 and u_1^1 . Concerning u_0^1 , we have by (25)-(26) that $g_{-1/2}^R = g_{-1/2}^R(u_{-1}^0, u_0^{1/2}) = g_{-1/2}^R(u^l, u^l) = g(u^l, u^l)$ and $g_{1/2}^L = g_{1/2}^L(u_0^{1/2}, u_1^0) = g_{1/2}^L(u^l, u^r) = g(u^l, u^l)$ since $(u^l, u^r) \in \mathcal{C}$ or $u^r = \varphi^b(u^l)$ by assumption. Then we get $u_0^1 = u_0^{1/2}$ by (23). Concerning u_1^1 , the values of $g_{1/2}^R$ and $g_{3/2}^L$ depend on if $u_1^{1/2} = u^l$ or $u_1^{1/2} = u^r$. If $u_1^{1/2} = u^l$, then $g_{1/2}^R = g_{1/2}^R(u_0^0, u_1^{1/2}) = g_{1/2}^R(u^l, u^l) = g(u^l, u^l)$ and $g_{3/2}^L = g_{3/2}^L(u_1^{1/2}, u_2^0) = g_{3/2}^L(u^l, u^r) = g(u^l, u^l)$ since $(u^l, u^r) \in \mathcal{C}$ or $u^r = \varphi^b(u^l)$. Similarly, if $u_1^{1/2} = u^r$, then $g_{1/2}^R = g_{1/2}^R(u_0^0, u_1^{1/2}) = g_{1/2}^R(u^l, u^r) = g(u^r, u^r)$ since $(u^l, u^r) \in \mathcal{C}$ or $u^r = \varphi^b(u^l)$, and $g_{3/2}^L = g_{3/2}^L(u_1^{1/2}, u_2^0) = g_{3/2}^L(u^r, u^r) = g(u^r, u^r)$. Then, $u_1^1 = u_1^{1/2}$ by (23).

We have thus proved that our algorithm is equivalent to Glimm's random choice scheme. The convergence towards the solution $u(x, t) = u^l$ for $x < \sigma(u^l, u^r)t$ and $u(x, t) = u^r$ for $x > \sigma(u^l, u^r)t$ is proved in [19] (see also [20]) as soon as the random sequence (a_n) is well distributed.

This completes the proof of the theorem.

4 Numerical experiments

In this section, we propose some numerical evidences in order to illustrate the relevance of the proposed transport-equilibrium strategy. To that purpose, we consider without loss of generality the cubic flux functions $f(u) = \varepsilon u^3$ with $\varepsilon = \pm 1$ which are to some extent the simplest examples of concave-convex ($\varepsilon = 1$) and convex-concave ($\varepsilon = -1$) functions. System (1) now reads

$$\begin{cases} \partial_t u + \partial_x \varepsilon u^3 = 0, & u(x, t) \in \mathbb{R}, \quad (x, t) \in \mathbb{R} \times \mathbb{R}^{+*}, \\ u(x, 0) = u_0(x). \end{cases} \quad (27)$$

Our objective is to compute the weak solutions of (27) satisfying the following entropy inequality

$$\partial_t u^2 + \frac{3}{2} \varepsilon \partial_x u^4 \leq 0, \quad (28)$$

that is $U(u) = u^2$ and $F(u) = \frac{3}{2} \varepsilon u^4$ in (6). Easy calculations lead to

$$\varphi^\sharp(u) = -\frac{u}{2} \quad \text{and} \quad \varphi_0^\flat(u) = -u,$$

so that (11) when $\varepsilon = 1$ and (12) when $\varepsilon = -1$ permit us (again without restriction) to consider a kinetic function of the form

$$\varphi^\flat(u) = -\beta^\varepsilon u, \quad \varphi^{-\flat}(u) = -\beta^{-\varepsilon} u, \quad (29)$$

with $\beta \in [1/2, 1)$. More precisely, we take $\beta = 3/4$. It is also easy to obtain

$$\rho(u, v) = -u - v \quad \text{and} \quad \varphi^\sharp(u) = (\beta^\varepsilon - 1)u.$$

Concerning the numerical flux g , we consider (again without restriction) a Relaxation scheme (see [14] for instance), that is

$$g(u, v) = \frac{1}{2}(f(u) + f(v)) - \frac{a(u, v)}{2}(v - u) \quad \text{with} \quad a(u, v) = \max(f'(u), f'(v)), \quad (30)$$

and following a proposal by Collela [9], we use the van der Corput random sequence (a_n) defined by

$$a_n = \sum_{k=0}^m i_k 2^{-(k+1)},$$

where $n = \sum_{k=0}^m i_k 2^k$, $i_k = 0, 1$, denotes the binary expansion of the integers $n = 1, 2, \dots$

Let us now validate our numerical strategy by first considering the typical behaviors of the Riemann solutions given in Section 2. We thus consider an initial data of the form (7).

When $f(u) = u^3$ (*i.e.* $\varepsilon = 1$), we take $u_l = 4$ and u_r respectively such that

Test A¹ : $u_r = 5$, *i.e.* $u_r > u_l$,

Test B¹ : $u_r = -0.5$, *i.e.* $u_r \in (\varphi^\sharp(u_l), u_l)$,

Test C¹ : $u_r = -2$, *i.e.* $u_r \in (\varphi^b(u_l), \varphi^\sharp(u_l))$,

Test D¹ : $u_r = -5$, *i.e.* $u_r < \varphi^b(u_l)$.

Numerical solutions are plotted on Figures 3 and 4.

When $f(u) = -u^3$ (*i.e.* $\varepsilon = -1$), we take $u_l = 3$ and u_r respectively such that

Test A⁻¹ : $u_r = 4$, *i.e.* $u_r > u_l$,

Test B⁻¹ : $u_r = 2$, *i.e.* $u_r \in (0, u_l)$,

Test C⁻¹ : $u_r = -1.5$, *i.e.* $u_r \in (\varphi^b(u_l), 0)$,

Test D⁻¹ : $u_r = -3$, *i.e.* $u_r < \varphi^b(u_l)$ and $u_l > \rho(\varphi^{-b}(u_r), u_r)$.

Numerical solutions are plotted on Figures 5 and 6.

The mesh used for these computations always contains 100 points per unit interval.

We observe that the numerical solutions fully agree with the exact ones. In simulations A¹ (Figure 3 - Left) and B⁻¹ (Figure 5 - Right), the solution is a single rarefaction wave remaining in a region of convexity and concavity of f , so that our algorithm exactly coincides with the Relaxation scheme (see theorem 1). It is the same for simulation A⁻¹ (Figure 5 - Left) for which the solution is a classical shock lying in a region of concavity of f . In simulation B¹ (Figure 3 - Right), the solution consists of a single classical shock wave, but connecting a convex region and a concave region of f , so that our two steps algorithm actually operates and provides by construction a sharp discontinuity. Basically, our algorithm exactly coincides with Glimm's random choice scheme for this test case (see theorem 1). In the last four Riemann problems (Figure 4 - Left and Right and Figure 6 - Left and Right), the solutions contain classical as well as nonclassical waves. Here again, we observe that the left and right states of the nonclassical waves are exactly captured while there are not any points in the corresponding profiles. The kinetic

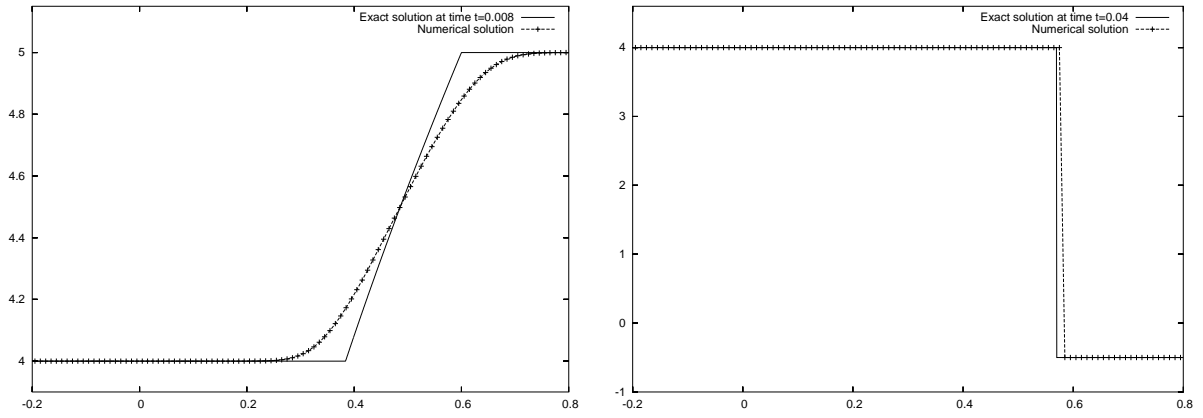


Figure 3: Classical solutions : test A¹ (Left) and B¹ (Right)

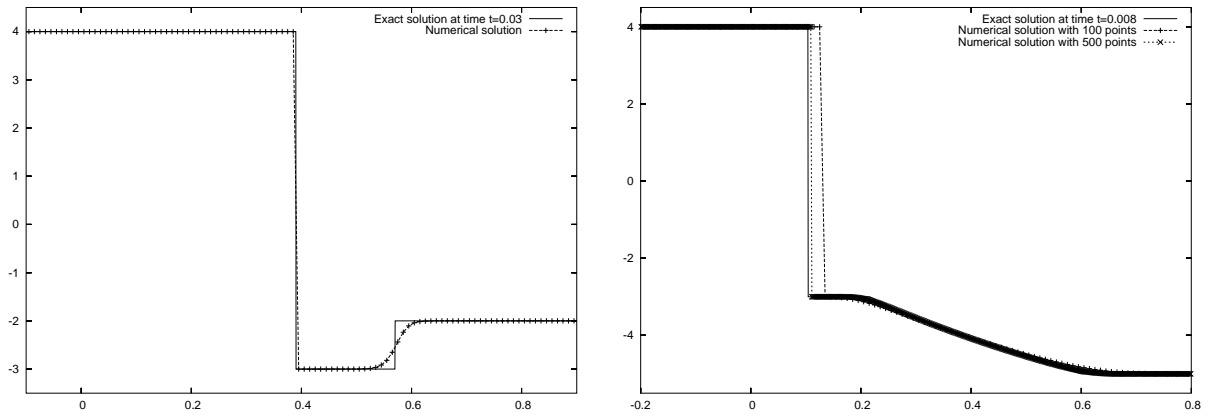


Figure 4: Nonclassical solutions : test C¹ (Left) and D¹ (Right)

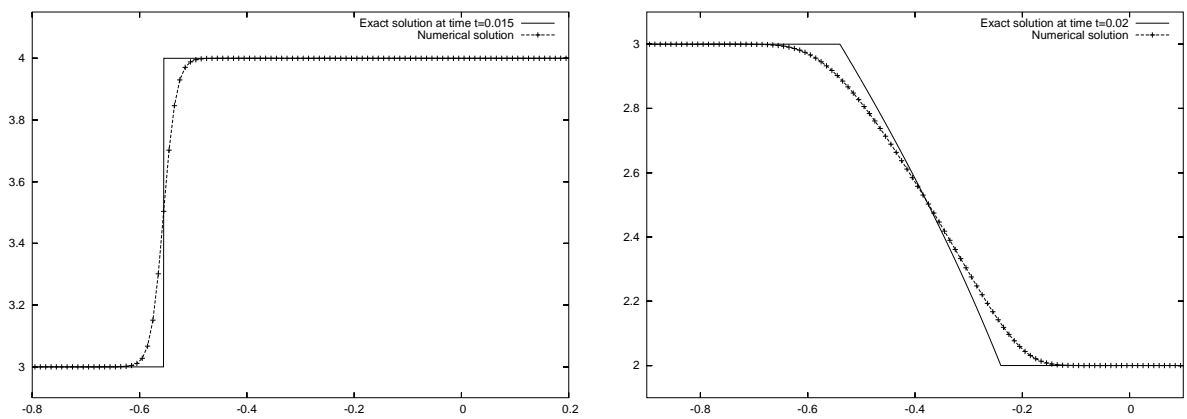


Figure 5: Classical solutions : test A⁻¹ (Left) and B⁻¹ (Right)

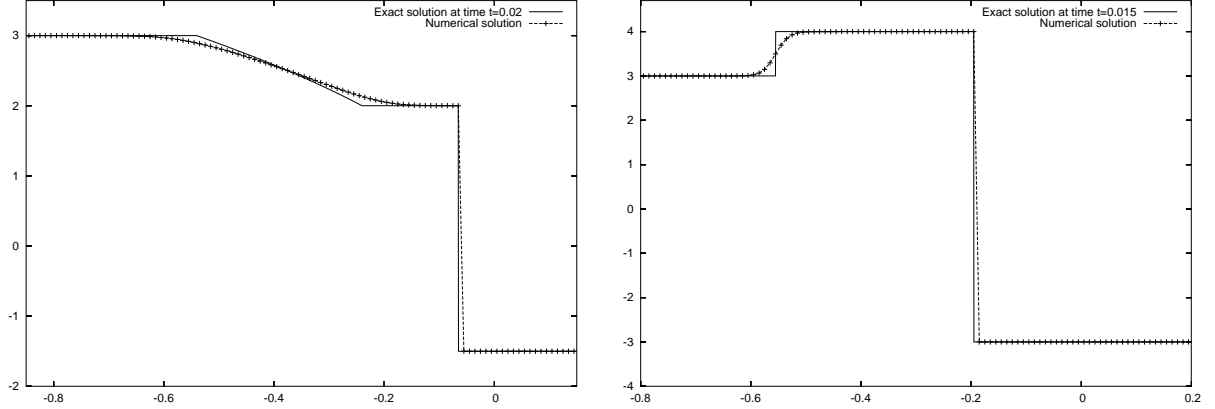


Figure 6: Nonclassical solutions : test C^{-1} (Left) and D^{-1} (Right)

criterion is respected perfectly. Note that for test D^1 , the numerical position of the nonclassical shock obtained with a 100-point mesh does not exactly coincide with the exact position (the difference is equivalent to three cells). Of course, this difference is due to the random sampling in the second step, and a better agreement is obtained with a mesh made of 500 points. Note that the numerical convergence towards the expected solution is proved in section 6 (actually for all the test cases considered here).

Remark 1 The reader may wonder why the concave-convex and convex-concave cases are treated separately despite an evident symmetry between these two situations at the continuous level. Our objective is to highlight that the numerical procedure is able to preserve such a symmetry. In particular, the method is able to create (if relevant) a nonclassical shock from u_l to $\varphi^b(u_l)$ in the concave-convex case, and from $\varphi^{-b}(u_r)$ to u_r in the convex-concave case. This deserves to be pointed out.

To conclude this section, we give an exemple of numerical solution provided by our method when the initial data is not a Riemann initial data (**Test E**). More precisely, we propose to consider

$$u_0(x) = \begin{cases} 1 & \text{if } x \leq -0.2, \\ -1 & \text{if } -0.2 \leq x \leq 0.2, \\ 1 & \text{if } x \geq 0.2, \end{cases}$$

together with $f(u) = u^3$ (without restriction). Periodic boundary conditions are used for this test case. For "small" times and locally around $x = -0.2$ and $x = 0.2$, the nonclassical solution consists of a nonclassical shock followed by a rarefaction wave (see section 2). Each wave propagates with a positive speed, they finally meet together to form a non self-similar solution. On figure 7, we show the solution at times $t = 0.07$ (a "small" time) and $t = 0.85$ (a "large" time), and for a mesh that contains 500 points. On table 1, we show for several meshes the ratio u_+/u_- associated with the two nonclassical shocks present in the solution (u_- and u_+ stand for the left and right states of the nonclassical shocks) at time $t = 0.85$. We can observe that it goes to -0.75 with the mesh size, which is nothing but the expected value. This case then further validates our method.

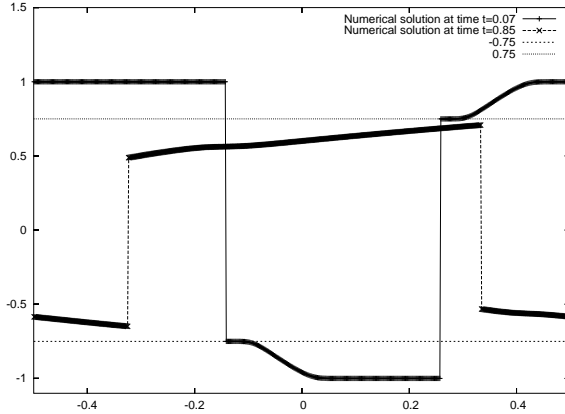


Figure 7: Periodic nonclassical solution : test E

Table 1: Discrete kinetic relation for the periodic nonclassical solution

# of points	First nonclassical shock	Second nonclassical shock
100	-0.7592859	-0.7580553
500	-0.7521835	-0.7515491
1000	-0.7509275	-0.7507187
2000	-0.7503732	-0.7503079

5 Towards sharp classical and nonclassical shocks

In this short section, we pay a particular attention to the cases C^1 , A^{-1} and D^{-1} . Figure 4 - Left, Figure 5 - Left and Figure 6 - Right show that the solution is composed of classical and/or nonclassical shocks. From a numerical point of view, we note that the nonclassical waves are sharp, while the classical ones are naturally diffused by the Relaxation scheme. The reason is that until now, we have only proposed a particular treatment for the nonclassical shocks since these are the most difficult to capture. If now we are also interested in computing sharp classical shocks (note that this point is not our objective in this paper), it turns out that it is sufficient to slightly modify the definitions of the numerical fluxes $g_{j+1/2}^L$ and $g_{j+1/2}^R$ in (25)-(26) so that all the shocks (classical as well as nonclassical) are kept at equilibrium during the second step. This is done by including classical shocks remaining in a same region of convexity of f in the definition of \mathcal{C} in (15). We get

$$\mathcal{C} = \tag{31}$$

$$\left| \begin{array}{l} \{(u_l, u_r) / u_l \varphi^\sharp(u_l) \leq u_l u_r < u_l^2\} \text{ if } f \text{ obeys (9),} \\ \{(u_l, u_r) / \{u_l^2 < u_l u_r\} \text{ or } \{u_l u_r \leq u_l \varphi^b(u_l) \text{ and } u_l^2 \leq u_l \rho(\varphi^{-b}(u_r), u_r)\}\} \text{ if } f \text{ obeys (10).} \end{array} \right.$$

Note that a related approach is more detailed and applied to systems of conservation laws in [5]. Figures 8 and 9 represent the numerical solutions obtained with this *modified* algorithm. As expected, both type of shocks are sharp.

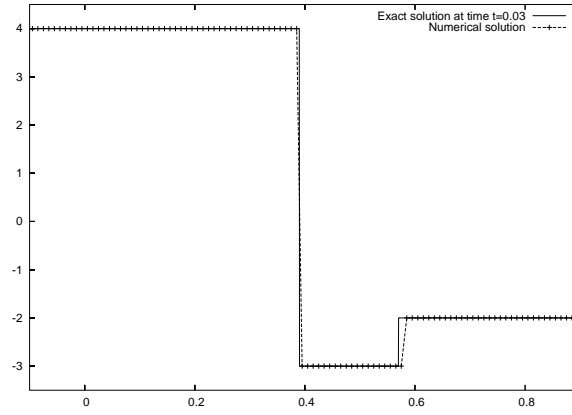


Figure 8: Nonclassical solution with the *modified* algorithm : test C^1

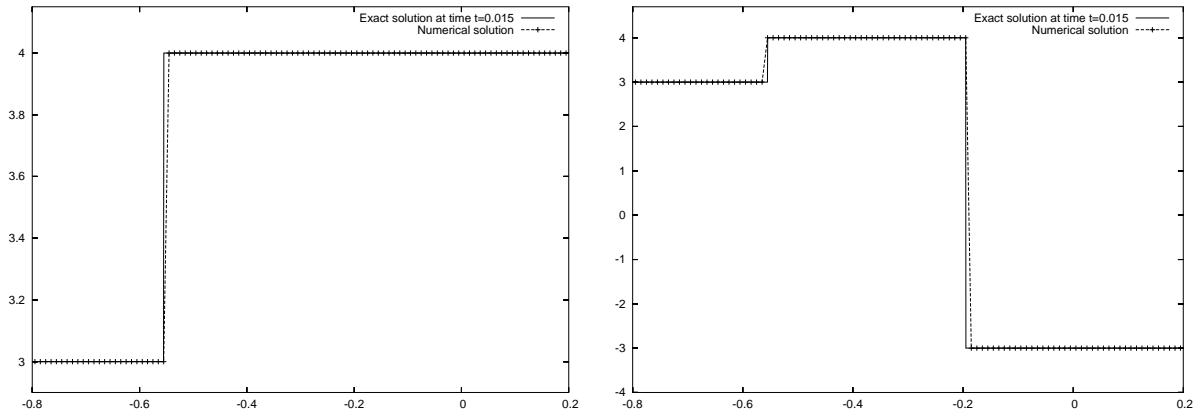


Figure 9: Nonclassical solution with the *modified* algorithm : test A^{-1} (Left) and D^{-1} (Right)

6 Conservation errors and convergence

The proposed transport-equilibrium algorithm is clearly nonconservative since the transport step is based on a random sampling strategy while two numerical fluxes g^L and g^R are used in the second step. In this section, we propose to measure the conservation errors on the numerical solution u_λ defined as

$$u_\lambda(x, t) = u_j^n \quad \text{if } (x, t) \in [x_{j-1/2}; x_{j+1/2}) \times [t^n; t^{n+1}).$$

Let us first recall that exact solution u evolves according to

$$\partial_t u + \partial_x f(u) = 0,$$

so that by integrating this equation between times $t = 0$ and $t = T > 0$ on the computational domain $[x_0, x_1]$ of \mathbb{R}_x , we easily get

$$\int_{x_0}^{x_1} u(x, T) dx - \int_{x_0}^{x_1} u_0(x) dx + \int_0^T f(u(x_1, t)) dt - \int_0^T f(u(x_0, t)) dt = 0. \quad (32)$$

Our objective is to get information about the validity of this equality at the discrete level. We propose for that to compare with 0 the function $E : T \in \mathbb{R}^+ \rightarrow E(T) \in \mathbb{R}$ with $E(T)$ defined by the relation

$$\begin{aligned} & \int_{x_0}^{x_1} u_\lambda(x, 0) dx \times E(T) = \\ & \int_{x_0}^{x_1} u_\lambda(x, T) dx - \int_{x_0}^{x_1} u_\lambda(x, 0) dx + \int_0^T f(u_\lambda(x_1, t)) dt - \int_0^T f(u_\lambda(x_0, t)) dt. \end{aligned} \quad (33)$$

Recall that u_λ is piecewise constant so that the evaluation of $E(T)$ does not raise any difficulty. In addition, it is worth noticing that if $f(u_\lambda(x_0, t))$ and $f(u_\lambda(x_1, t))$ coincide for all $t \in [0, T]$ with the corresponding exact values $f(u(x_0, t))$ and $f(u(x_1, t))$ (this is in particular the case when the dynamics of the numerical solution did not reach yet the boundaries x_0 and x_1 of the computational domain) and that $u_\lambda(x, 0)$ and u_0 are the same (this is true for a Riemann initial data for instance), then (33) reduces to

$$E(T) = \frac{\int_{x_0}^{x_1} u_\lambda(x, T) dx - \int_{x_0}^{x_1} u(x, T) dx}{\int_{x_0}^{x_1} u_\lambda(x, 0) dx},$$

in view of (32). In other words, $E(T)$ represents the relative conservation error of u at time T on interval $[x_0, x_1]$. In the next table 2, we give for tests B¹, C¹, D¹, C⁻¹ and D⁻¹ the values of the L^1 -norm $\frac{1}{T_f} \|E\|_{L^1(0, T_f)}$ of E , namely

$$\frac{1}{T_f} \|E\|_{L^1(0, T_f)} = \frac{1}{T_f} \int_0^{T_f} |E(T)| dT = \sum_{t^n=0}^{t^{n+1}=T_f} \frac{(t^{n+1} - t^n)}{T_f} |E(t^{n+1})|,$$

where T_f is the final time of the corresponding simulations presented in section 4. We will consider four different meshes containing 100, 500, 1000 and 2000 points per unit interval. The computational domain $[x_0, x_1]$ is $[-0.2, 0.8]$ for tests B¹, D¹, $[-0.1, 0.9]$ for test C¹, $[-0.85, 0.15]$ for test C⁻¹, $[-0.8, 0.2]$ for test D⁻¹ and $[-0.5, 0.5]$ for test E. Note that for the other tests cases,

Table 2: Relative conservation errors.

# of points	Test B ¹	Test C ¹	Test D ¹	Test C ⁻¹	Test D ⁻¹	Test E
100	$1.12e^{-1}$	$2.96e^{-2}$	$4.77e^{-2}$	$4.95e^{-3}$	$4.21e^{-2}$	$3.20e^{-2}$
500	$9.00e^{-3}$	$4.47e^{-3}$	$1.24e^{-2}$	$1.25e^{-3}$	$1.15e^{-2}$	$7.15e^{-3}$
1000	$4.50e^{-3}$	$2.38e^{-3}$	$6.03e^{-3}$	$8.00e^{-4}$	$6.92e^{-3}$	$3.71e^{-3}$
2000	$2.25e^{-3}$	$1.14e^{-3}$	$3.23e^{-3}$	$3.67e^{-4}$	$3.56e^{-3}$	$2.13e^{-3}$

the method reduces to the Relaxation scheme so that the method is actually conservative (no conservation error is made). We observe that the conservation errors are small even when the mesh is pretty coarse, and decrease towards 0 with the mesh size.

Finally and for the sake of completeness, we provide in table 3 another quantitative evaluation of our method through the L^1 -norm between the exact and the numerical solutions. We observe that these errors tend to zero with the mesh size for all the test cases, which proves numerically the convergence of the method.

Table 3: L^1 errors.

# of points	Test A ¹	Test B ¹	Test C ¹	Test D ¹
100	$2.98e^{-2}$	$4.50e^{-2}$	1.51	0.248331
500	$9.60e^{-3}$	0.	$1.70e^{-2}$	$5.38e^{-2}$
1000	$5.67e^{-3}$	0.	$8.51e^{-3}$	$3.48e^{-2}$
2000	$3.28e^{-3}$	0.	$4.26e^{-3}$	$1.79e^{-2}$
# of points	Test A ⁻¹	Test B ⁻¹	Test C ⁻¹	Test D ⁻¹
100	$1.64e^{-2}$	$2.41e^{-2}$	$5.98e^{-2}$	$1.64e^{-2}$
500	$3.29e^{-3}$	$7.22e^{-3}$	$2.14e^{-2}$	$1.73e^{-2}$
1000	$1.59e^{-3}$	$4.16e^{-3}$	$7.73e^{-3}$	$1.56e^{-2}$
2000	$7.95e^{-4}$	$2.36e^{-3}$	$2.39e^{-3}$	$7.80e^{-3}$

7 Conclusion

We have presented a new powerful numerical strategy for approximating nonclassical solutions whose dynamics is dictated by a kinetic function. The main idea was the modification of a given conservative scheme in order to make correctly computed the underlying undercompressive waves. We have seen that our algorithm reduces sometimes to Glimm's random choice scheme, and sometimes to the basic conservative scheme. Actually, our algorithm keeps the advantages of Glimm's random choice scheme without its drawbacks since first, it does not depend on the knowledge of the (nonclassical) Riemann solution, and then it provides sharp interfaces propagating at the right speed. The strategy is moreover strongly consistent with the continuous model in the sense of Theorem 1. However, proving some additional stability properties (like the convergence towards the expected nonclassical solution, or even a TV bound) remains an open

question. The next step is to propose an extension of the method to the case of systems. Note that in [4], we apply our numerical strategy to approximate the possibly nonclassical solutions of a macroscopic model for the description of the flow of pedestrians.

References

- [1] Amadori D., Baiti P., LeFloch P.G. and Piccoli B., *Nonclassical shocks and the Cauchy problem for non-convex conservation laws*, J. Differential Equations, vol 151, pp 345-372 (1999).
- [2] Botchorishvili R., Perthame B. and Vasseur A., *Equilibrium schemes for scalar conservation laws with stiff sources*, INRIA research report No 3891 (2000).
- [3] Chalons C., *Bilans d'entropie discrets dans l'approximation numérique des chocs non classiques. Application aux équations de Navier-Stokes multi-pression 2D et à quelques systèmes visco-capillaires*, PhD Thesis, Ecole Polytechnique, (2002).
- [4] Chalons C., *Numerical approximation of a macroscopic model of pedestrian flows*, Preprint of the Laboratoire Jacques-Louis Lions (2005).
- [5] Chalons C. and Coquel F., *Capturing infinitely sharp discrete shock profiles with the Godunov scheme*, submitted.
- [6] Chalons C. et LeFloch P.G., *A fully discrete scheme for diffusive-dispersive conservation laws*, Numerisch Math., vol 89, pp 493-509 (2001).
- [7] Chalons C. et LeFloch P.G., *High-order entropy conservative schemes and kinetic relations for van der Waals fluids*, J. Comput. Phys., vol 167, pp 1-23 (2001).
- [8] Chalons C. et LeFloch P.G., *Computing undercompressive waves with the random choice scheme. Nonclassical shock waves*, Interfaces and Free Boundaries, vol 5, pp 129-158 (2003).
- [9] Collela P., *Glimm's method for gas dynamics*, SIAM J. Sci. Stat. Comput., vol 3, pp 76-110 (1982).
- [10] Hayes B.T. and LeFloch P.G., *Nonclassical shocks and kinetic relations : Scalar conservation laws*, Arch. Rational Mech. Anal., vol 139, pp 1-56 (1997).
- [11] Hayes B.T. and LeFloch P.G., *Nonclassical shocks and kinetic relations : Finite difference schemes*, SIAM J. Numer. Anal., vol 35, pp 2169-2194 (1998).
- [12] Hou T.Y., LeFloch P.G. and Rosakis P., *A Level-Set Approach to the Computation of Twinning and Phase Transition Dynamics*, J. Comput. Phys., vol 150, pp 302-331 (1999).
- [13] Hou T.Y., LeFloch P.G. and Zhong X., *Converging Methods for the Computation of Propagating Solid-Solid Phase Boundaries*, J. Comput. Phys., vol 124, pp 192-216 (1996).
- [14] Lattanzio C. and Serre D., *Convergence of a relaxation scheme for hyperbolic systems of conservation laws*, Numer. Math., vol 88, pp 121-134 (2001).
- [15] LeFloch P.G., *Propagating phase boundaries: formulation of the problem and existence via the Glimm scheme*, Arch. Rational Mech. Anal., vol 123, pp 153-197 (1993).

- [16] LeFloch P.G., **Hyperbolic Systems of Conservation Laws: The theory of classical and nonclassical shock waves**, E.T.H. Lecture Notes Series, Birkhäuser (2002).
- [17] LeFloch P.G. and Rohde C., *High-order schemes, entropy inequalities, and nonclassical shocks*, SIAM J. Numer. Anal., vol 37, pp 2023-2060 (2000).
- [18] LeFloch P.G. and Shearer M., *Nonclassical Riemann solvers with nucleation*, Proc. Royal Soc. Edinburgh, vol 134A, pp 941-964 (2004).
- [19] Liu T.P., *The deterministic version of the Glimm scheme*, Comm. Math. Phys., vol 57, pp 135-148 (1977).
- [20] Serre D., **Systèmes de lois de conservation**, Diderot éditeur, Arts et Sciences (1996).